Design and Simulation of Modular Multilevel Converter Fed Induction Motor Drive

Ahmed K. Hannan[1], Turki K. Hassan[2]
[1,2]Electrical Engineering Department, College of Engineering, Mustansiriah University, Iraq

Article Info	ABSTRACT

Traditional modular multilevel converter (MMC) applications in medium voltage induction motor drive are difficult, particularly at low speeds because of the higher amplitude of the voltage ripple of the sub-module capacitor. This paper uses a hybrid MMC to achieve a lower peak-to-peak voltage ripple of the sub-module capacitor particularly at low frequencies. The vector control strategy with the closed-loop speed control is used to indicate an accurate and wide-speed range. MATLAB / Simulink is used to simulate and obtain the simulation results of hybrid and traditional MMC with induction motor drive and compare from the standpoint of capacitor voltage ripple. The results are shown the reduction of peak-to-peak voltage ripple of the sub-module capacitor as the hybrid MMC is operated.

Corresponding Author:

Ahmed K. Hannan,
Electrical Engineering Department,
Mustanisirah University,
Baghdad, Iraq.
Email: ahmedkamilh69@gmail.com

1. INTRODUCTION

Multilevel converter topologies in the power electronic industries are generally accepted as one of the latest technological advances. One of its applications with variable speed motor drive due to its higher performance [1-2]. Therefore the modular multilevel converters in recent years are become efficient topology in high and medium-power applications because of their efficiency, modularity, low redundancy expense, scalability [3-6]. They have reshaped power transmission systems based high voltage source converters (VSC-HVDC) [7, 8], and are considered to be the key technology for developing successful DC Super Grids [9]. They are used in the medium-voltage motor drive applications in recent years [10-16]. MMC presents more advantages in relation to the three most widely used topologies [17, 18], namely flying capacitor (FC), neutral point clamping (NPC), and cascaded H Bridges (CHB) as shown in Figure 1 [19]. MMC has major advantages: it can easily increase the number of levels without increased control complexity or unequal distribution of losses and does not need costly and bulky isolation transformers.

Despite the advantages of the MMC. The peak-to-peak capacitor voltage ripple is one of the main problems that appeard in the variable speed drive applications, which must be taken into consideration. The peak-to-peak capacitor voltage ripple will increase when the motor operates at a low speed. This because that the capacitor voltage ripple is inversely proportional to the frequency and is proportional to the ampiltued of the load current, and also the value of the sub-module (SM) capacitor should be taken into consideration [20]. Therefore it is difficult to drive the motor at low speeds with constant torque.

This paper suggests a hybrid topology by adding a controllable series switch that connects between the MMC and the DC bus voltage. The main advantage of this topology is to reduce the peak-to-peak voltage ripple of the SM capacitor, specifically at low motor speeds. In this paper, the hybrid MMC is used to drive a medium voltage induction motor, also the vector control strategy is used to get accurate speed control. Lower peak-to-peak voltage ripple of the SM capacitor can be observed when hybrid MMC is used compared with traditional MMC.
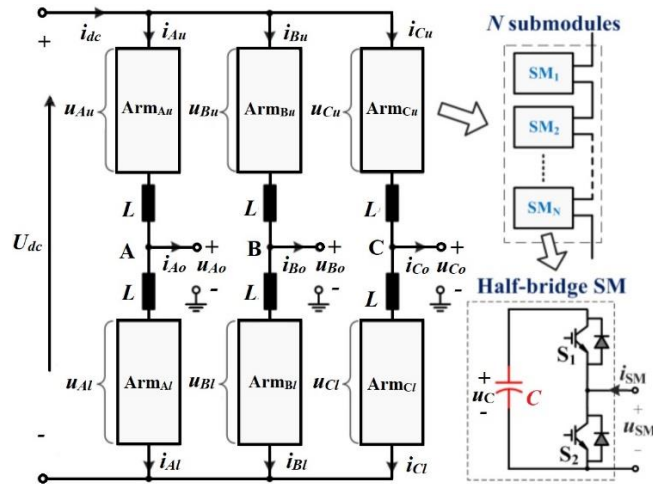
Figure 1. MMC circuit diagram

2.   THE HYBRID MMC: ANALYSIS AND OPERATION

Figure 2 shows the suggested hybrid MMC circuit diagram. A controllable series switch is applied between the MMC and the DC-bus voltage in order to minimize the average arm voltages of the MMC, leading to minimize capacitor voltage ripples [21]. The thyristor and IGBT can be used as this switch. In additional, a snubber circuit [22] is required to filter the harmonics of the switching voltage. The converter can be grounded to the earth by two grounding resistors R_g. The three-phase MMC circuit as well-known, each phase includes two arms (upper and lower) are attached by two buffer inductors L; each arm includes N identical half bridge SMs which are connected in series to build the output voltage stepwise, and SM has a capacitor with average voltage of U_{dc}/N . The output voltage term is u_{jo} in phase of j (j∈{A,B,C}), the output current is i_{jo}, and the DC bus voltage is U_{dc}, and the MMC dc terminal voltage is u_d, the upper and lower arm voltages are u_{ju} and u_{jl} respectively, the upper and lower arm currents are i_{ju} and i_{jl} respectively.
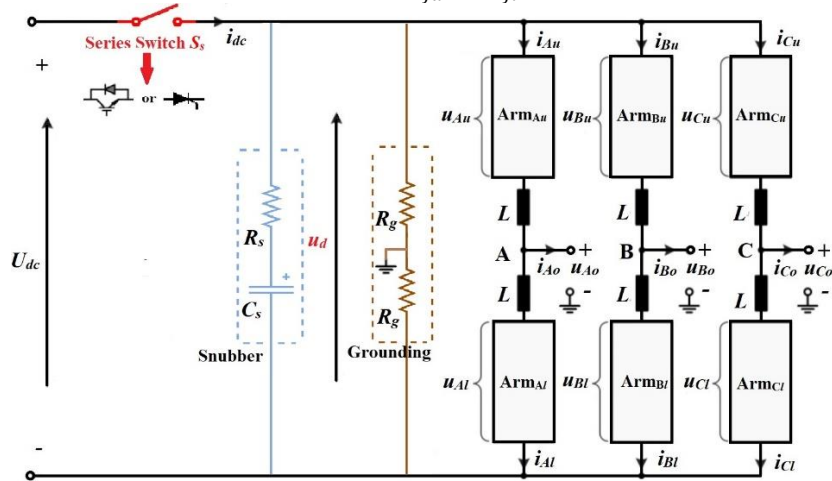

Figure 2. Circuit diagram of hybrid MMC [23]

The upper and lower currents of the MMC can be expressed as:

$$\begin{cases} i_{ju} = i_{cj} + {}^1\!/_2\, i_{jo} \\ i_{jl} = i_{cj} - {}^1\!/_2\, i_{jo} \end{cases} \tag{1}$$

Where i_{cj} represents the circulating current inside the arms of phase j. The MMC output voltages and currents can be expressed as:

$$\begin{aligned} u_{jo} &= U_O\ \cos(\omega t + \delta_j) \\ i_{jo} &= I_O\ \cos(\omega t + \delta_j - \varphi) \end{aligned} \tag{2}$$

Where δ_j is the phase angle of the output ($\delta_A = 0^\circ, \delta_B = 120^\circ, \delta_C = 240^\circ$), and the angular frequency is ω, and the phase lag angle is φ, and the magnitudes of the output voltage and current are U_O and I_O respectively. The magnitude of the output voltage can be expressed as:

$$U_O = {}^1/_2 \, m \, U_{dc} \tag{3}$$

Where the modulation index ratio is m, which represents V/f ratio and adjusting between 0-1. It must be approximately ensured constant when the converter used in variable-speed drive application, the modulation index can be written as:

$$m = \frac{\omega}{\omega_{rated}} \tag{4}$$

The average arm voltages of the MMC per phase can be written as:

$$u_{ju} = {}^1/_2 \, U_{dc}(1 - m\cos(\omega t))$$
$$u_{jl} = {}^1/_2 \, U_{dc}(1 + m\cos(\omega t)) \tag{5}$$

When the power balance between the DC side and ac output side is achieved, the rated DC current I_{dc} component can be expressed as:

$$I_{dc} = {}^3/_4 \, m \, I_O \, \cos\varphi \tag{6}$$

2.2. Operation Principle of Hybrid MMC

Figure 3 shows the operation principle of the hybrid MMC. When the series switch is switched on, the dc terminal voltage u_d equal to U_{dc}. When the series switch is switched off, the dc terminal voltage u_d of MMC is minimized to twice of the output voltage amplitude $(2U_O)$ per phase, this leads to reduce the capacitor voltage ripple. The switching frequency of series switch is f_h ($f_h = 1/T_h$) is 10 times of the output voltage frequency f_o [23]. The DC currents of the hybrid MMC are expressed as:

$$I_{dc} = \begin{cases} I_{dc(rated)}, & if \ (S_s = 1) \\ 0, & if \ (S_s = 0) \end{cases} and \ i_c = \frac{1}{3} i_{dc} \tag{7}$$

Based on (3), the expression of dc terminal voltage u_d is:

$$u_d = \begin{cases} U_{dc}, & if \ (S_s = 1) \\ m \, U_{dc}, & if \ (S_s = 0) \end{cases} \tag{8}$$

The average dc terminal of u_d is:

$$\bar{U}_d = DU_{dc} + (1 - D)mU_{dc} \tag{9}$$

The arm voltages of hybrid MMC for phase A are [23]:

$$\begin{cases} u_{ju} = {}^1/_2 \, u_d - {}^1/_2 \, m \, U_{dc} \cos(\omega t) - \Delta u_d \\ u_{jl} = {}^1/_2 \, u_d + {}^1/_2 \, m \, U_{dc} \cos(\omega t) - \Delta u_d \end{cases} \tag{10}$$
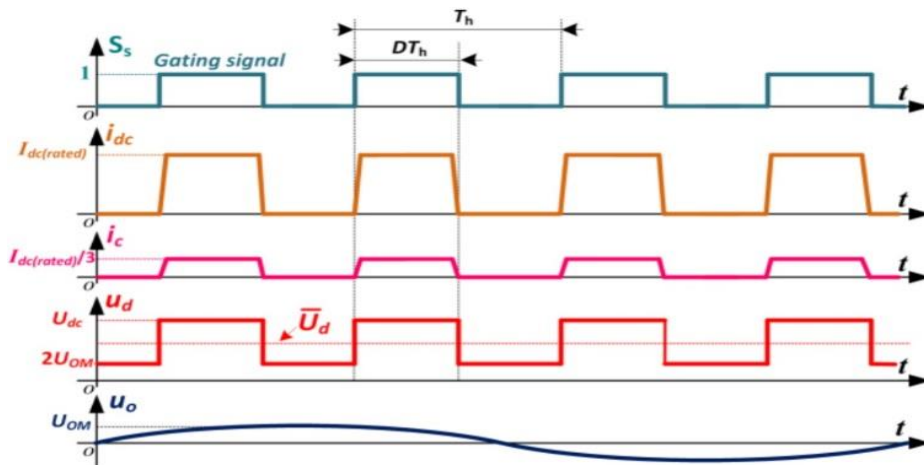

Figure 3. Hybrid MMC Sketch waveforms [24]

Where Δu_d is used to control the circulating current i_c. The balancing of the active power between ac and dc terminals can be achieved by varying the duty cycle D: ($U_{dc}I_{dc(rated)}D = \frac{3}{2}U_O I_O \cos\varphi$), the balance

must be occurred when the motor speed varies. Hence the duty cycle D can be derived for constant torque drives with $I_O = I_{O(rated)}$ [25].

$$D = m = \frac{\omega}{\omega_{rated}} \tag{11}$$

The peak-to-peak voltage ripple of The SM capcitor of hybrid MMC in [23] can be expressed as:

$$\Delta U_{C(pp)} = \left(2 - \frac{\omega}{\omega_{rated}}\right)\frac{I_{O(rated)}}{2\omega_{rated}C} \tag{12}$$

Where the capacitance of SM is C. The capacitor voltage ripple of traditional MMC can be obtained by [19]:

$$\Delta U_{C(pp)} = \frac{I_O}{2\omega C} \tag{13}$$

3. CONTROL SCHEME

Figure 4 shows the suggested control scheme for hybrid MMC to drive the induction motor based on vector control strategy, it includes of five main blocks, that are the series switch control block, circulating current control block, induction motor vector control block, the SM balancing control block, and the phase-shifted carrier PWM(PSC-PWM).
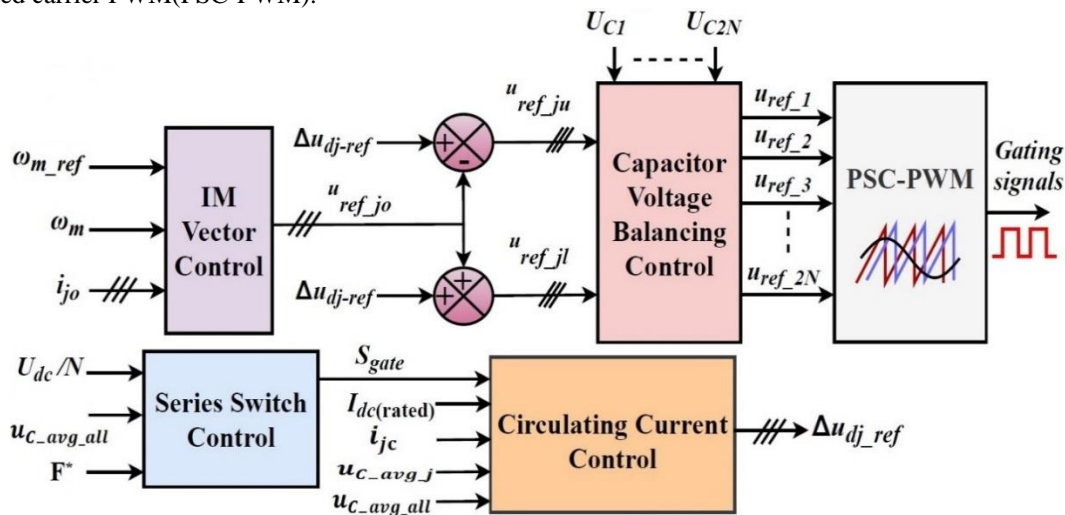

Figure 4. The suggested control scheme for hybrid MMC

3.1. Series Switch Control Block

The power balance between dc input and ac output must be achieved to ensure a stable operation of the hybrid MMC. It is necessary to measure the average voltage of the SMs capacitors ($U_{C\_all(avg)}$) to keep it equal to U_{dc}/N as a reference value because the difference between the input and output powers would affect the stored energy in the capacitors. So the duty cycle D is adjusted for this purpose as shown in figure 5 [23]. The $U_{C\_all(avg)}$ represents the dc average voltage of all the SMs capacitors. To obtain the dc average voltage of the SMs capacitors, the SM capacitor voltages of the upper and lower arms must be calculated, it can be expressed as [26]:

$$u_{C\_avg\_ju} = \sum_{i=1}^{N} u_{cap\_ju}(i) \tag{14}$$

$$u_{C\_avg\_jl} = \sum_{i=1}^{N} u_{cap\_jl}(i) \tag{15}$$

Subsequently, the average voltage of SMs capacitors in phase j is obtained [27]

$$u_{C\_avg\_j} = \frac{1}{2N}\sum_{i=1}^{2N} u_{cap\_j}(i) \tag{16}$$

The $u_{C\_avg\_all}$ is obtained by summation the average voltage of the SMs capacitors in phase j. it can be expressed as [28]:

$$u_{C\_avg\_all} = \frac{1}{3}\sum u_{C\_avg\_j} \tag{17}$$

Due to the sensitivity of PI controller to the harmonics, a moving average filter (MAF) is used to obtain the dc average voltage of the SMs capacitor.
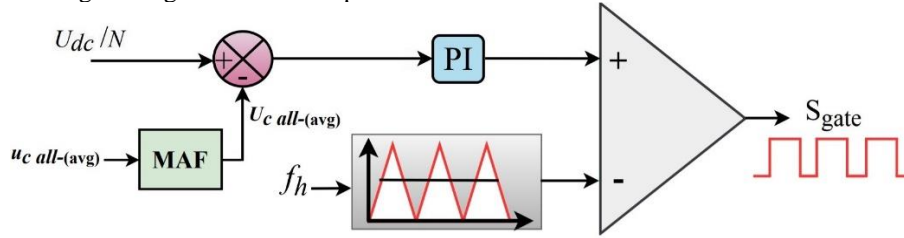

Figure 5. Series switch control block [23]

3.2. Circulating Current Control Block

The stored energy in each phase j must be kept balanced by modifying the dc component of the circulating current [23]. As shown in Figure 6, the dc average voltage of all SMs capacitors of three-phase ($U_{C\_all(avg)}$) is compared with the dc average voltage of SMs capacitors in phase j ($U_{C(avg-j)}$). PI control is used to minimize this voltage variation and to produce a dc circulating current ΔI_{jc}. After that, this current added to the $1/3 I_{dc(rated)}$ component to obtain I_{c-ref}. It is necessary to multiply I_{c-ref} by the duty cycle, and the circulating current reference will be obtained [23]. The aim of that is to force the actual circulating current to follow I_{c-ref}. Thus the controlled variable is Δu_d. So the circulating current control is used for this purpose.
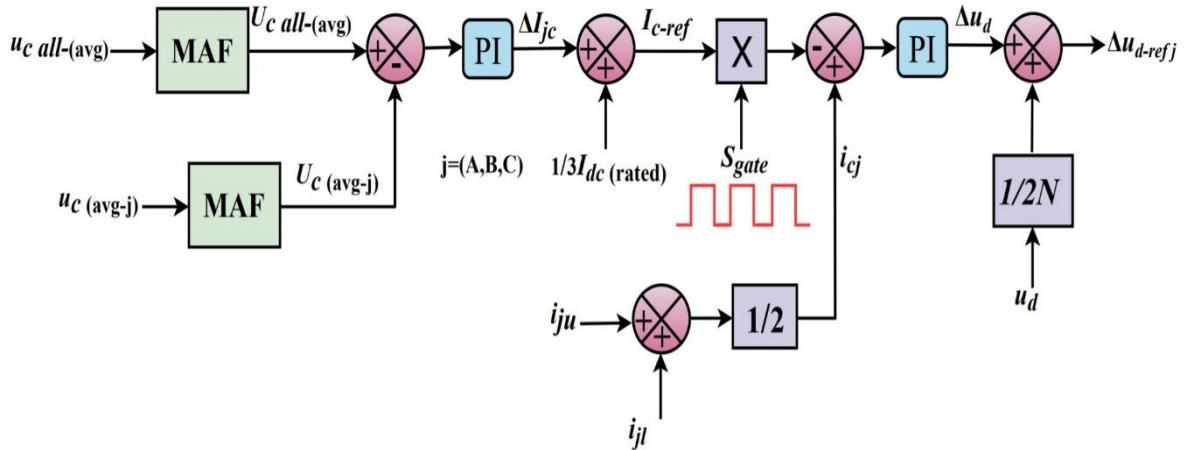

Figure 6. Circulating current control [23]

3.3. Vector Control Block

Vector control is a high-efficiency control strategy that similar to the DC machine speed control system [29]. Figure 7 shows the implementation of vector control fed induction motor. The motor speed ω_m is compared to the desired speed ω_{m_ref} in the speed control loop, and the error is applied to PI control to produce i_{qs_ref}. In i_{qs} control loop the i_{qs_ref} is compared to the i_{qs} which is equivalent to the output torque, and the error is applied to PI control to obtain u_{q_ref}. In flux control loop the flux of the motor ψ_r is compared to the desired flux ψ_{r_ref}, obtaining the i_{ds_ref} which compared to the i_{ds} to obtain u_{d_ref} using PI controllers. The motor excitation can be controlled from the id control loop. Finally, the generated (d-q) voltages are converted to reference output voltages (ABC) by inverse Clarke-Park transformation. The mathematical equations [30]:

$$\psi_r = \frac{L_m}{T_r P + 1} i_{ds} \tag{18}$$

$$\omega_{sl} = \frac{L_m i_{qs}}{T_r \psi_r} \tag{19}$$

$$\omega_s = \omega_r + \omega_{sl} \tag{20}$$

$$\theta_e = \int \omega_s \, d_t \tag{21}$$

Where T_r is the time constant ($T_r = L_r / R_r$), ω_{sl} is the angular slip speed, p is the differential operator and θ_e is the rotor flux angle, and ω_s is the synchronous speed.
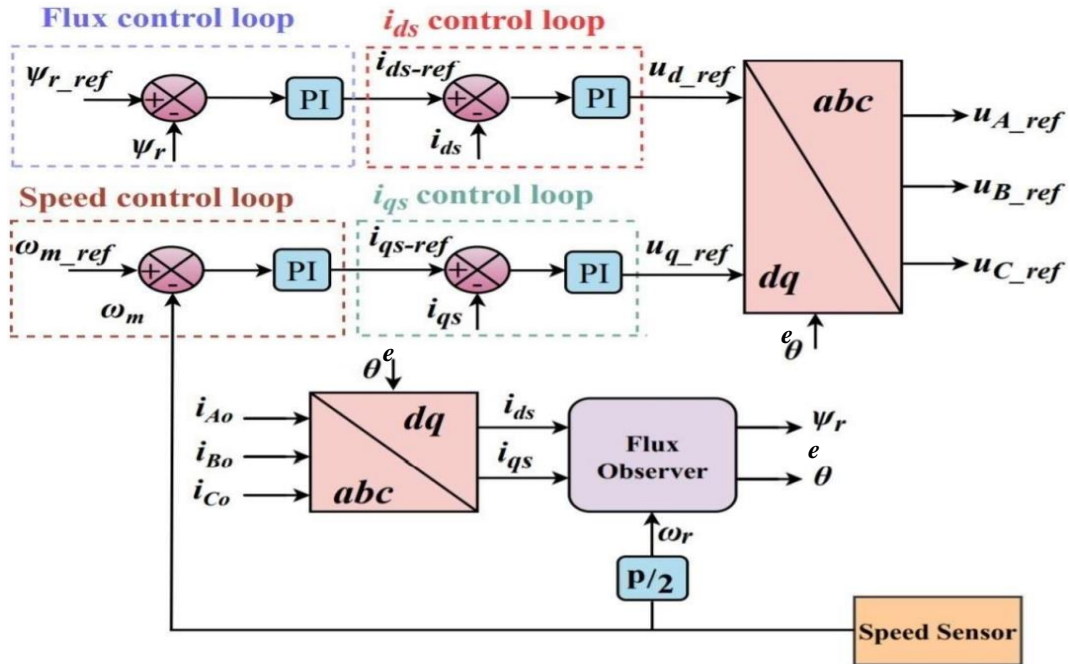
Figure 7. Vector control of induction motor block

Subsequently, the references arms voltages u_{ju_ref} and u_{jl_ref} in Figure 4 are applied to the SM balancing control block to balance the SMs capacitor voltages.

3.4. Capacitor Voltage Balancing Control Block

When the SM is activated, current would be pass through the SM causes the charge and discharge and the capacitor voltage fluctuation occurs. Due to the difference in switching time in each sub- module, the capacitor voltage in the same arm is imbalanced [27]. So the capacitor voltage balancing control is used to avoid the imbalance of the capacitor voltage. Figure 8 shows the implementation of the capacitor voltage balancing control blocks for upper and lower arms. This method is different compared to individual-balancing listed in [31]. The upper and lower arm reference voltages can be expressed as [26]:

$$u_{ref-ju}(i) = \frac{u_{ref-ju}}{N} + K_p(\frac{u_{C-avg\_ju}}{N} - u_{cap-ju}(i)) \times \text{sign}(i_{ju}) \qquad (22)$$

$$u_{ref-jl}(i) = \frac{u_{ref-jl}}{N} + K_p(\frac{u_{C-avg\_jl}}{N} - u_{cap-jl}(i)) \times \text{sign}(i_{jl}) \qquad (23)$$

Where K_p represents the proportional gain, "$sign(x)$" denotes signum function it can be written as:

$$sign(x) = \begin{cases} 1 & , \ x \geq 0 \\ -1 & , x < 0 \end{cases} \qquad (24)$$

The produced references $u_{ref-ju}(i)$ and $u_{ref-jl}(i)$ will be applied to the PWM modulator to generate the gate control pulses for the semiconductor switches to build the voltage stepwise
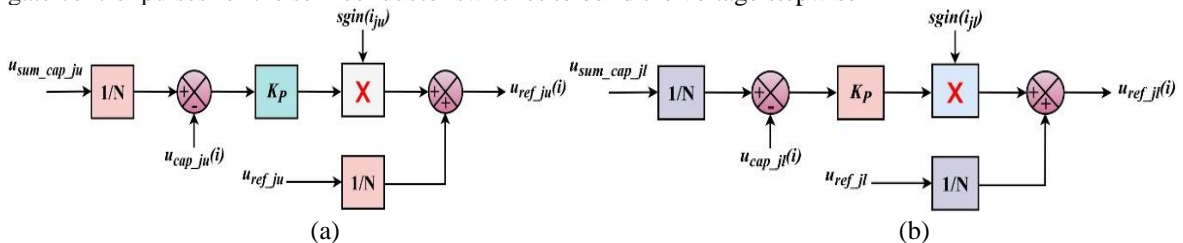

Figure 8. The capacitor voltage balancing control [26], (a) upper arm, (b) lower arm

3.5. The Phase-Shifted Carrier PWM Block

Phase-shifted PWM technique is another comprehensive multi-carrier modulation since it improves the equivalent switching frequency and minimize the harmonics of output voltage and easy to design. This

method requires N identical triangular carriers with the amplitude of U_{dc}/N. Each sub-module have a triangular carrier with frequency of f_c, and the phase displacement between them is $2\pi/N$. Carriers of the phase-shifted PWM are shown in Figure 9. Figure 10 shows the Block diagram of the Phase-shifted PWM.
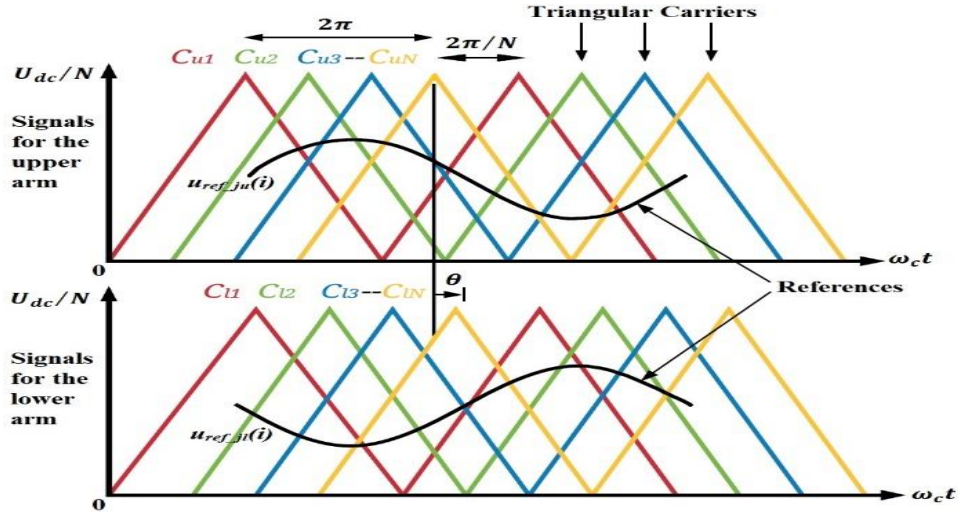

Figure 9. Phase-shifted carriers [16]

Where θ is the displacement angle of the carriers between the upper and lower arm. For power electronic converters, the higher equivalent switching frequency and lower harmonic content of the output voltage mean that the required filter components are smaller and cost less. The lowest output voltage harmonic content of MMC can be obtained by selecting the displacement angle as follows [16]:

$$\theta = \begin{cases} 0 & , N \text{ is odd} \\ \frac{\pi}{N} & , N \text{ is even} \end{cases} \tag{25}$$
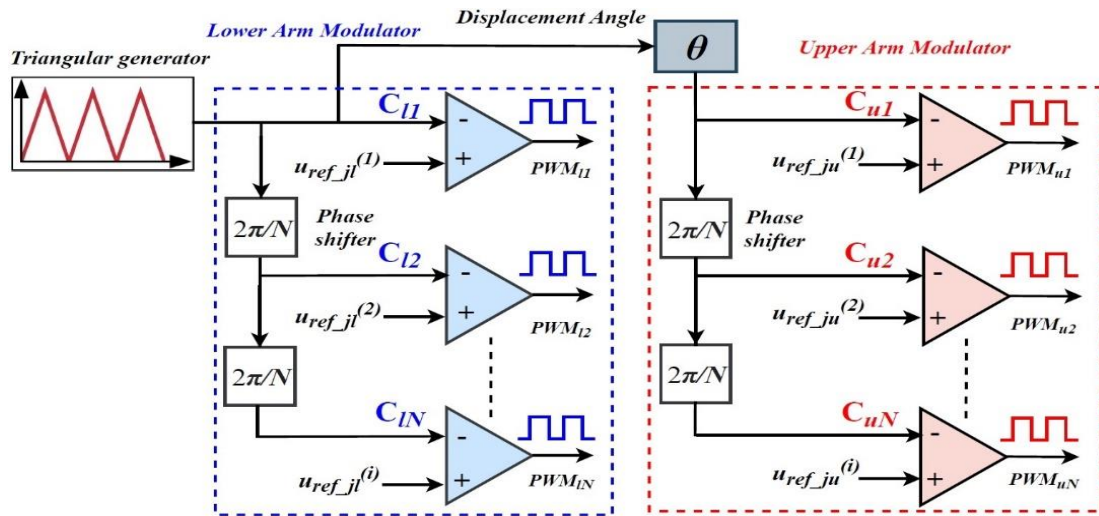

Figure 10. Phase-shifted PWM block diagram

4. SIMULATION AND RESULTS

To evaluate the effectiveness of the proposed hybrid MMC, a 1MW, 4160V hybrid MMC is simulated in MATLAB/Simulink environment, with ten half-bridge SMs per arm. Detailed parameters of the proposed converter are listed in Table I. In order to verify the dynamic performance of hybrid MMC, a 6-pole 4.16kV/1MW three phase induction motor (IM) with a constant load torque, was simulated, with the motor parameters in Table I. The hybrid MMC was simulated under three cases to show the reduction of peak-to-peak voltage ripple of the SM capacitor and compared with the traditional MMC. The feasibility of the suggested system is verified by comparing it with the system in [23].

Table 1. Simulation Parameters

Hybrid MMC parameters

Parameters	Value
Number of SMs per arm N	10
DC-source voltage U_{dc}	7kV
Nominal SM capacitor voltage U_C	700V
SM capacitance C_{SM}	4000µF
Arm inductance L	1mH
Rated output frequency $f_{o(rated)}$	60Hz
Rated phase current I_O	212A
PSC-PWM frequency f_c	1kHz
S_s switching frequency f_h	$10 \times f_o$
Snubber resistance	200Ω
Snubber capacitance	1µF
IM parameters	
Parameters	Value
Rated active power P_s	1250hp
Number of pole pairs pp	3
Rated speed ω_m	1200 rpm
Rated line-to-line voltage U_{rated}	4160V
Stator rms current I_O	150A
Power factor $\cos\varphi$	0.968
Mechanical load torque T_{rated}	7490N.m
Stator Flux linkage ψ_s	9Wb
Stator resistance R_s	0.21Ω
Rotor resistance R_r	0.146Ω
Stator leakage inductance L_{ls}	5.2mH
Rotor leakage inductance L_{lr}	5.2mH
Magnetizing Inductance L_m	155mH
Moment of Inertia J	47.6kg-m^2

4.1. Case 1:

In this case, the hybrid MMC is operated the same as a traditional MMC, the induction motor operates at rated speed of 1189 rpm and no-load torque, after 2 second period a step load torque 7490N.m is applied to the induction motor as shown in Figure 11 (a), the motor speed remains the same as before this because the PI controller returns it to the reference value as shown in Figure 11 (b). The increase of the load torque leading to increase the quadrature current i_{qs} which is proportional to the output torque while the direct current i_{ds} remains constant since the flux is constant as shown in Figure 12 (a). Figure 12 (b) shows the increase of the stator currents amplitude from 50A to its rated value of 212A. The DC-bus current i_{dc} will increase from 37Amp to 147Amp as shown in Figure 13 (a). Due to the increase of output current the arm currents i_{Au}, i_{Al} are increased from 37 Amp to 155 Amp which are approximate equal to ($\frac{1}{2}I_{jo} + \frac{1}{3}I_{dc}$) as shown in Figure 13 (b), also the peak–to–peak voltage ripple of the SM capacitor is inceased from 25V to 55V with average voltage of U_{dc}/N (700V), this because of equation (13) as shown in Figure 14 (a). The output voltage of the converter with rated frequency at stady state to fit the rated motor speed is shown in Figure 14 (b).
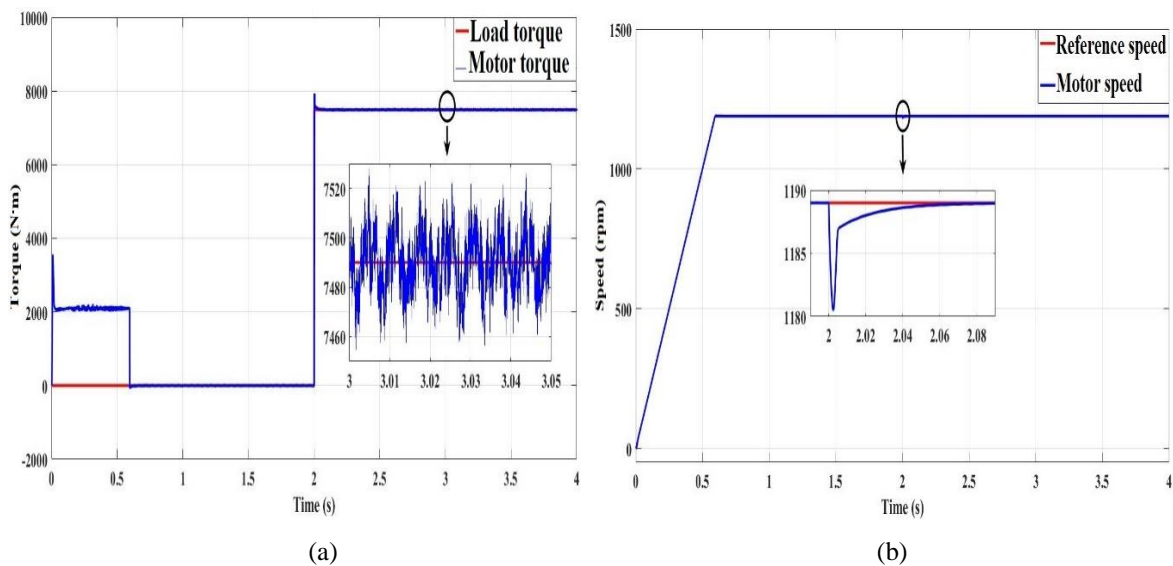

(a)   (b)

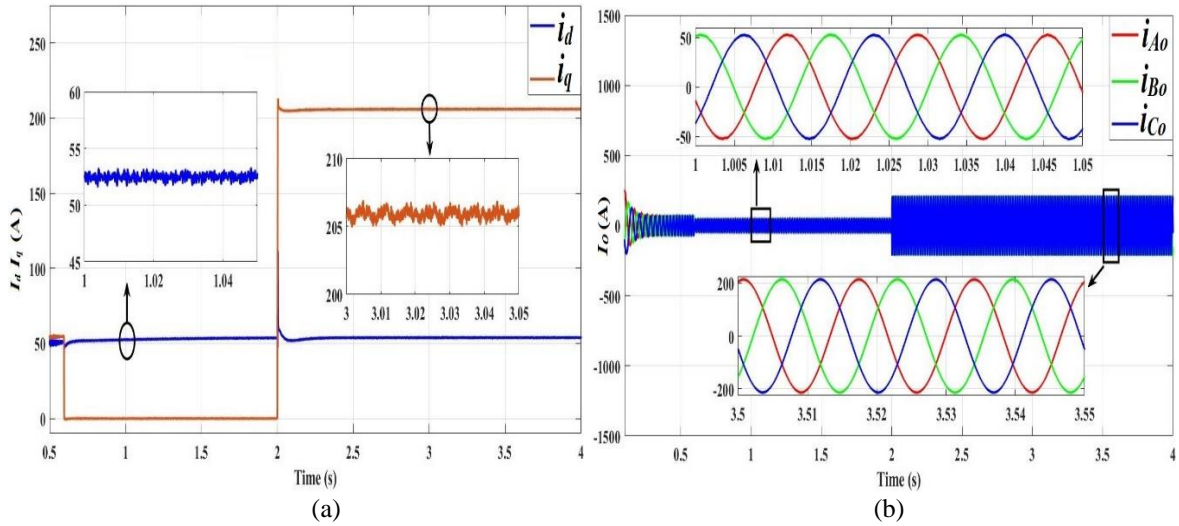Figure 11. Simulation results of case 1 (a) motor load torque, (b) motor speed

(a)   (b)

Figure 12. Simulation results of case 1 (a) I_d and I_q current component of the motor, (b) motor stator currents

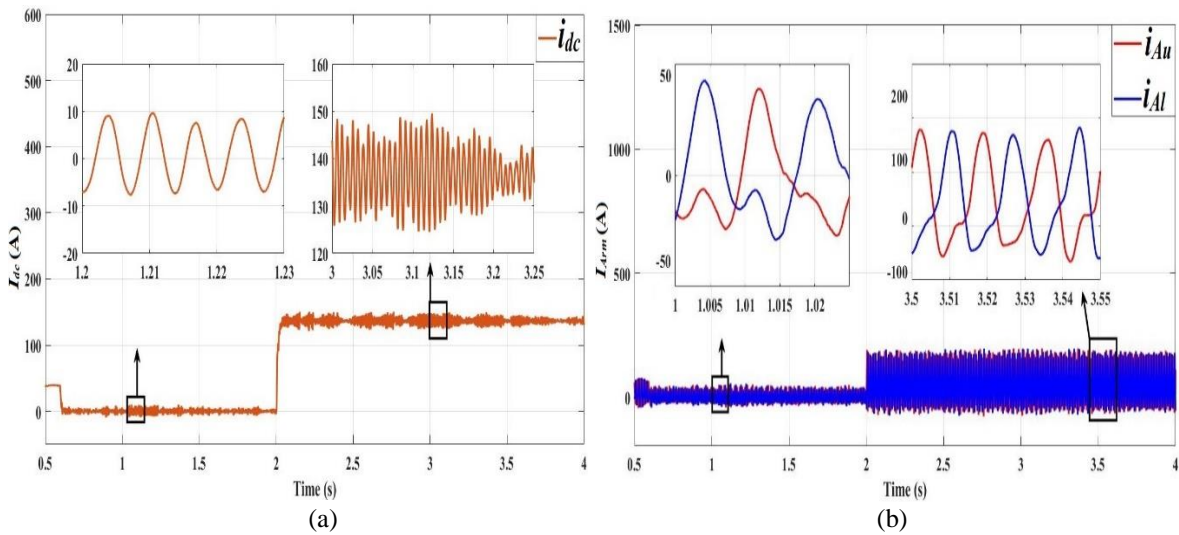(a)   (b)

Figure 13. Simulation results of case 1 (a) DC-bus current, (b) Arm current of phase A

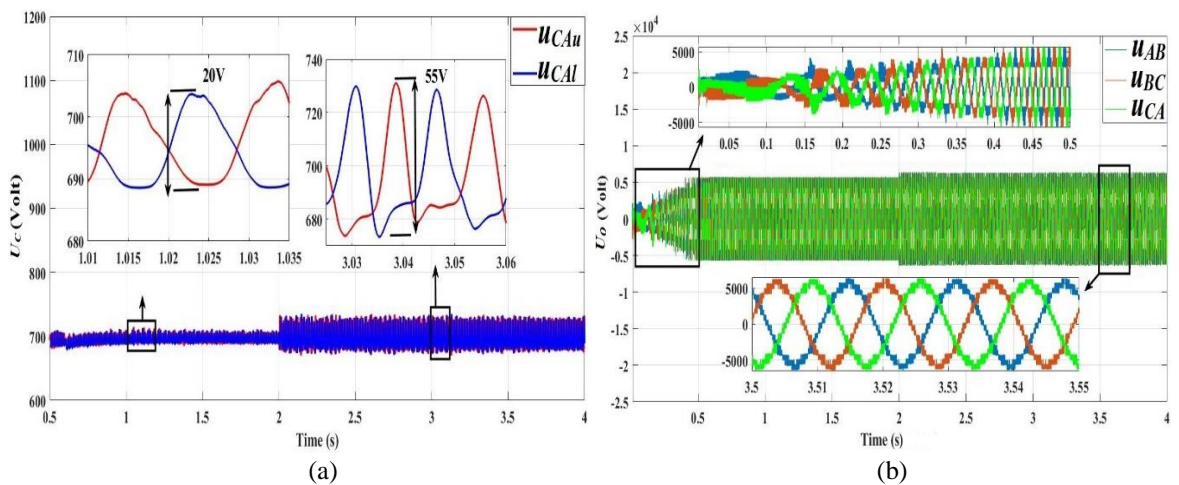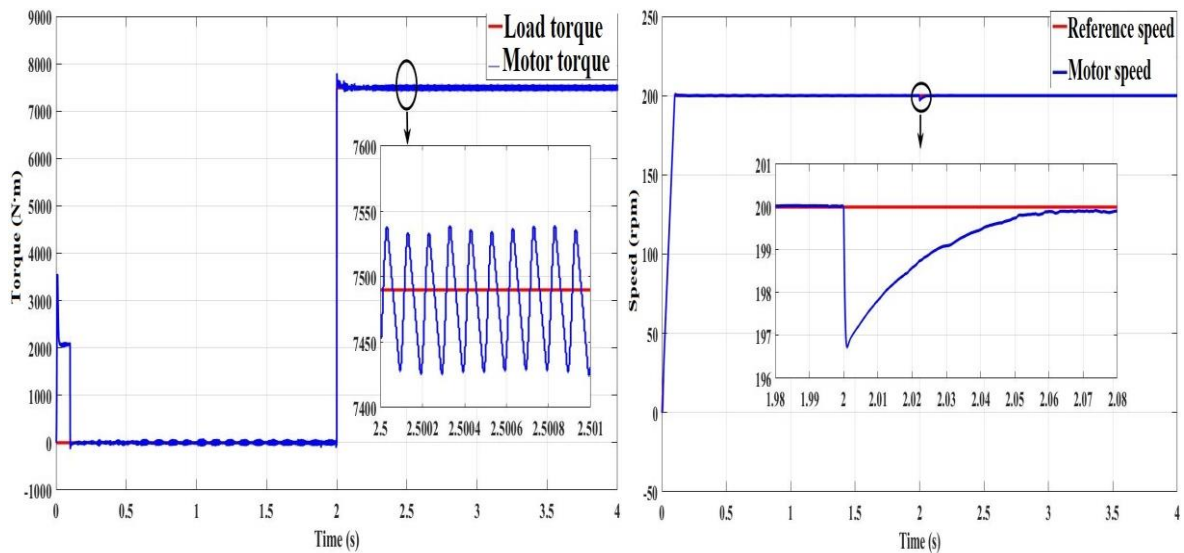(a)   (b)

Figure 14. Simulation results of case 1 (a) SM capacitor voltages of phase A, (b) Converter output voltages

4.2. Case 2:

In this case, the hybrid MMC is operated as a traditional and hybrid MMC, the motor is operated at low speed of 200 rpm, at 2 second period a step load torque is increased from zero to its rated value of 7490

N.m as shown in Figure 15 (a). Figure 15 (b) shows a good-dynamic performance of vector control to get accurate speed control and return the motor speed to its reference value when the load is changed. As the load torque is increased the quadrature current i_{qs} is also incresed as shown in Figure 16 (a). Figure 16 (b) shows increase the stator currents amplitudes form 50A to 212A with high-quality sinusoidal waveforms. Figure 17 (a) shows the gate signal of the series switch S$_S$ that appeared after each time period of 0.01 second, this means that the switching frequency f_h of the series switch is equal to 100Hz($10 \times f_o$), also the dc termial voltage u_d is appeared after each time period of 0.01 as shown in Figure 17 (b). As the output current is increased the DC-bus current and arm currents are also increased to their ratied value as shown in Figure 18 (a) and Figure 18 (b) respectively. Figure 19 (a) shows the peak-to-peak voltage ripple of the SMs u_{cAu} u_{cAl} of the traditional MMC significantly increases from 115V to 432V with average value of 700V this because equation (13). If the operating frequency is further reduced, the voltage ripple of the capacitor will become extremely large, causing the entire converter to fail to operate normally, while the average value of the SM capacitor voltage of hybrid MMC is stable at 700V and increased from 40V to 140V this because equations (12). Also, there is a good response of voltage balancing control to keep the balance between the SMs capactior during the load change. Most importantly, compared to Figure 19 (b), the SM capacitor voltage ripple reduction was 292V, which proves that the hybrid MMC has lower capacitor voltage ripple. The converter output voltage with frequency of 10Hz at stady state to get the desired speed is shown in Figure 20.

(a)   (b)

Figure 15. Simulation results of case 2 (a) motor load torque, (b) motor speed.
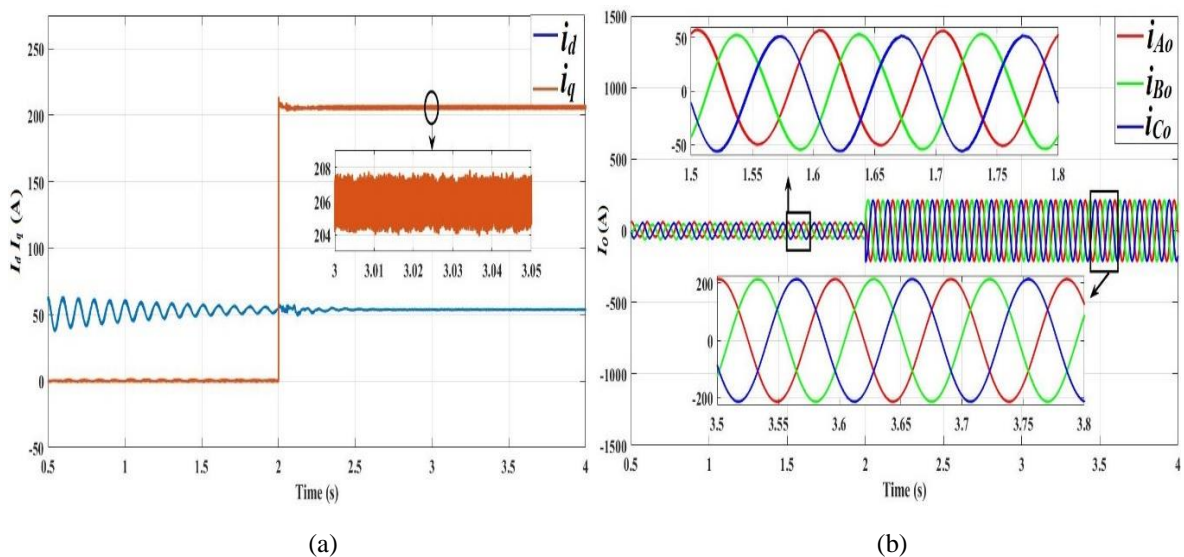
(a)   (b)

Figure 16. Simulation results of case 2 (a) I_d and I_q current component of the motor, (b) motor stator currents
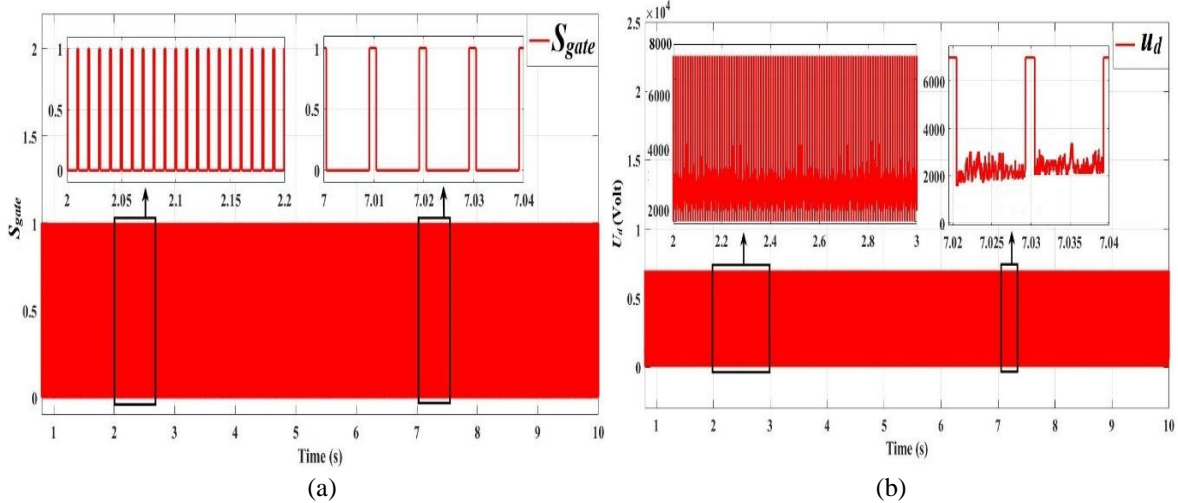
(a) (b)
Figure 17. Simulation results of case 2 (a) Sgate, (b) dc terminal voltage
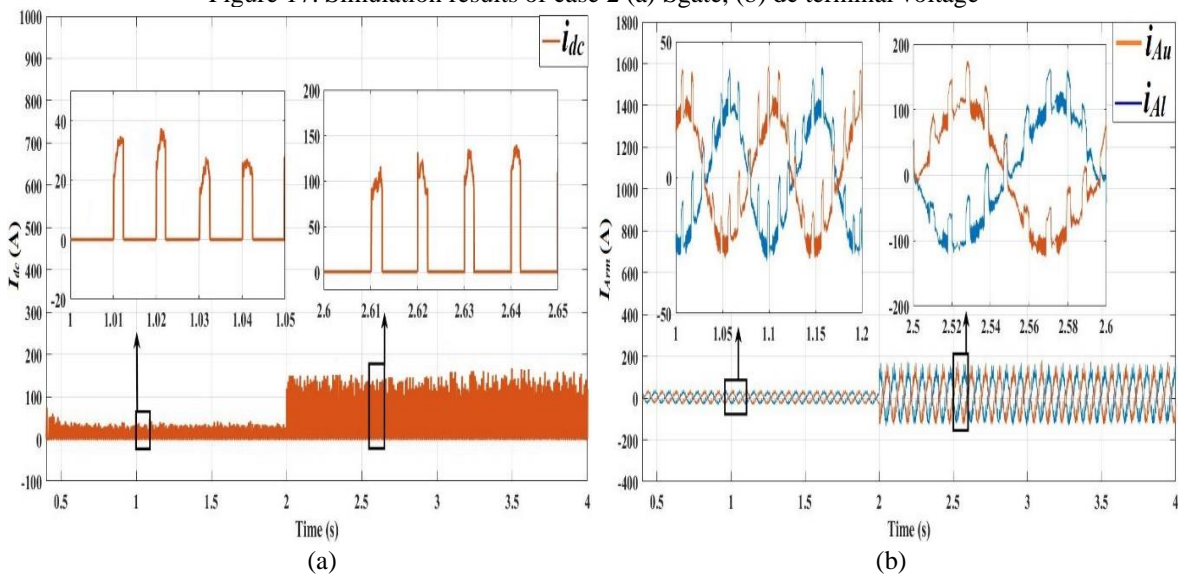

(a) (b)
Figure 18. Simulation results of case2 (a) DC-bus current, (b) Arm current of phase A
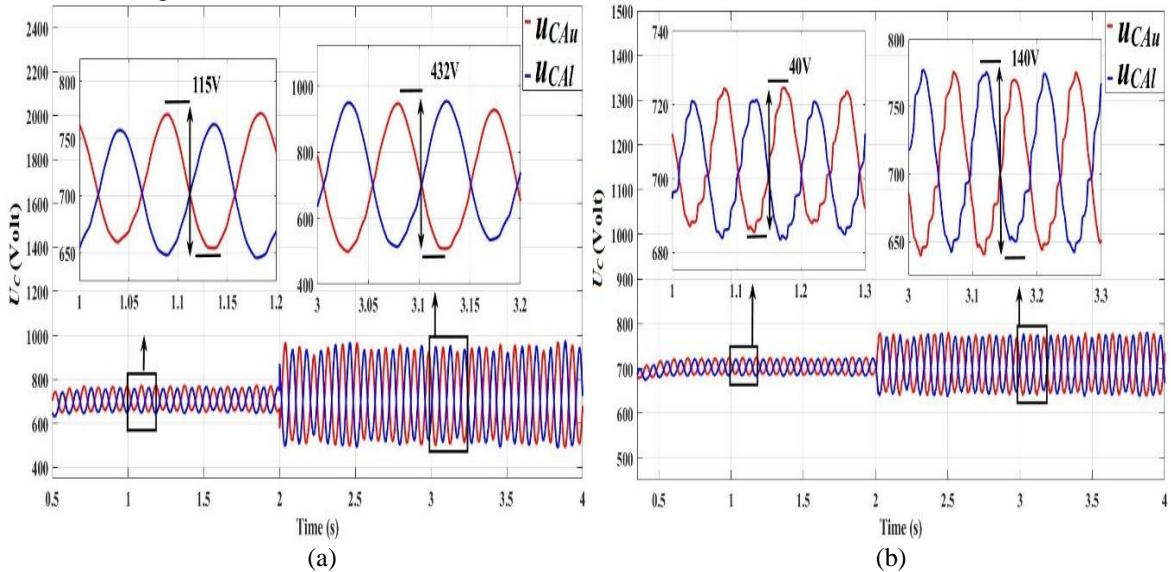

(a) (b)
Figure 19. Simulation results of case2 (a) traditional MMC SM capacitor voltages of phase A, (b) hybrid MMC SM capacitor voltages of phase
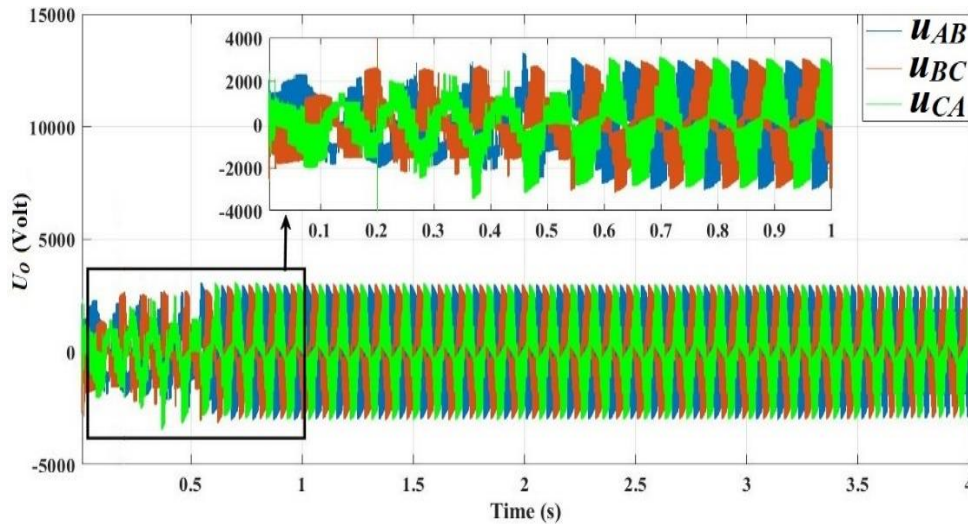
Figure 20. Converter output voltages

4.3. Case 3:

In this case, the hybrid MMC is operated at very low frequency (5Hz) to show its ability for reduction of capacitor voltage ripple. The motor is operated with very low speed of 100rpm, and the load torque is increased from zero to 7490N.m at 4 second period as shown in Figure 21 (a). The motor speed is maintained with the reference value because of the closed loop speed control as shown in Figure 21 (b). The i_{qs} component follows the load torque and has a value which is proportional with the output torque while the direct current i_{ds} remains constant since the flux is constant as shown in Figure 22 (a). Figure 22 (b) shows the increasing the stator currents amplitudes form 50A to 212A with high-quality sinusoidal waveforms. Since the output frequency is 5Hz, this means that the series switch is operated at frequency of 50Hz as shown in Figure 23 (a), also the dc termial votage u_d is appeared after each time period of 0.02 as shown in Figure 23 (b). Since the load torque is increased the DC-bus current and arm currents are also increased to their ratied value as shown in Figure 24 (a) and Figure 24 (b) respectively. Figure 25 (a) shows the peak-to-peak voltage ripple of the SM capacitor u_{cAu} u_{cAl} of the traditional MMC that significantly increases from 225V to 860V with average value of 700V. In practice this required to increase the size of the capacitor, leading to increase cost, therefor it is difficult to drive the motor at low speed with traditional MMC. Compared with traditional MMC the peak-to-peak capacitor voltage ripple, the hybrid MMC can operate with a lower peak-to-peak capacitor voltage ripple with 60V to 170V at the same speed as shown in Figure 25 (b). The converter output voltages are set to get the required motor speed as shown in Figure 26.
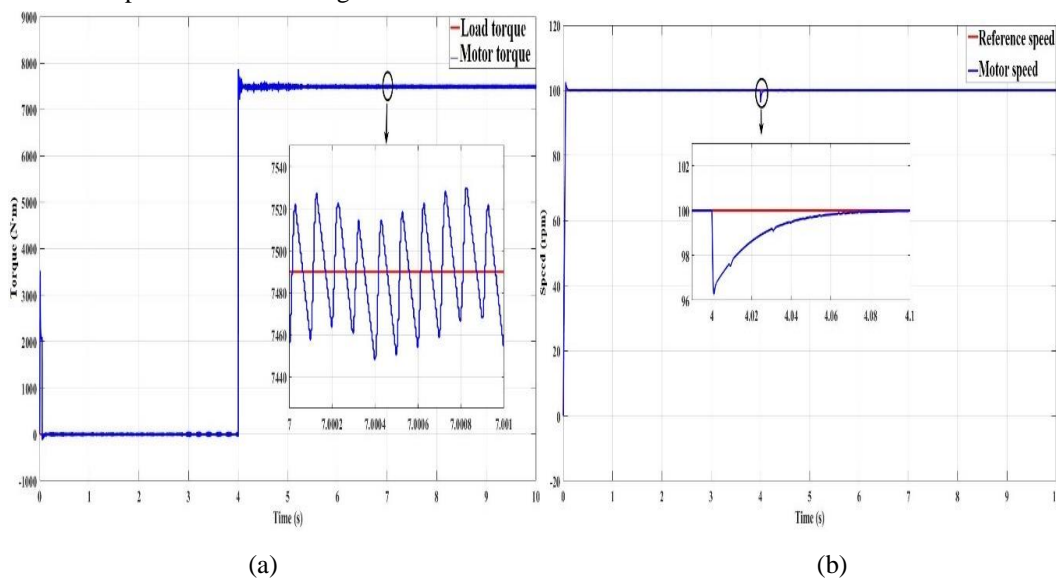

(a)   (b)

Figure 21. Simulation results of case 3 (a) motor load torque, (b) motor speed.
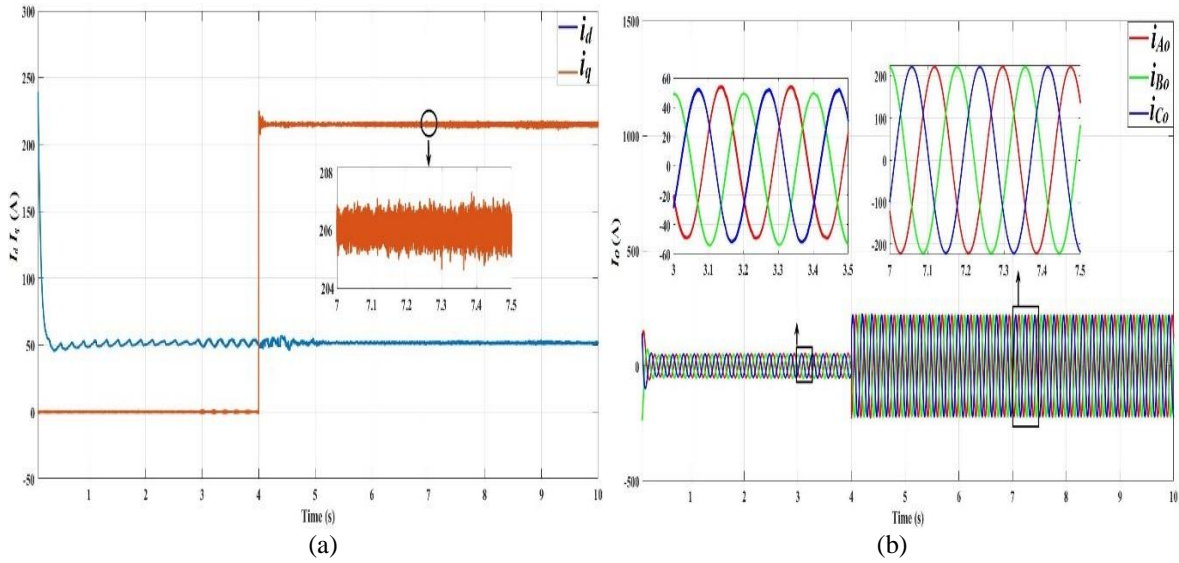
(a)   (b)

Figure 22. Simulation results of case 3 (a) I_d and I_q current component of the motor, (b) motor stator currents

(a)   (b)

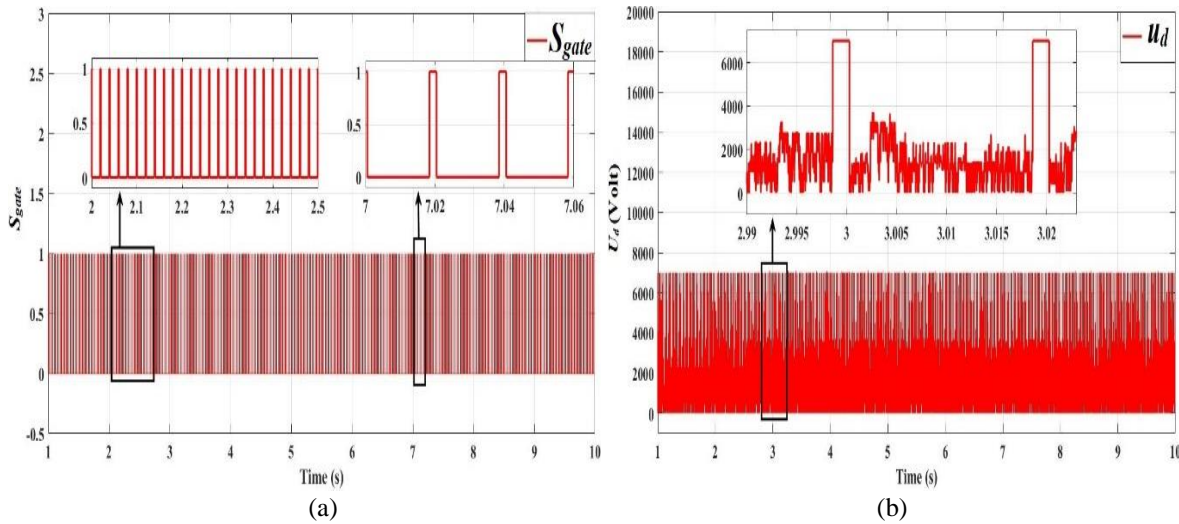Figure 23. Simulation results of case 3 (a) Sgate, (b) dc terminal voltage

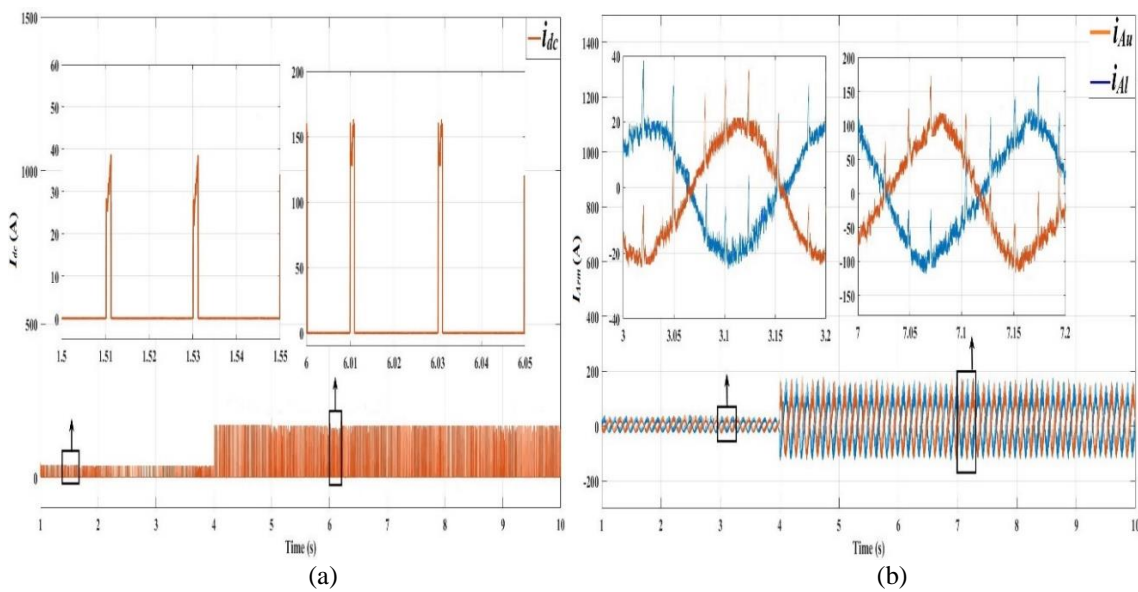(a)   (b)

Figure 24. Simulation results of case 3 (a) DC-bus current, (b) Arm current of phase A

(a)   (b)
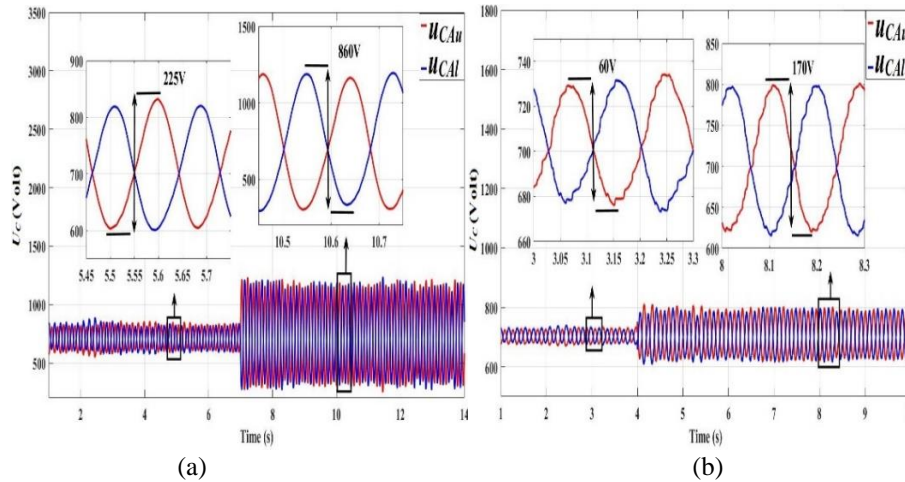
Figure 25. Simulation results of case2 (a) traditional MMC SM capacitor voltages of phase A, (b) hybrid MMC SM capacitor voltages of phase
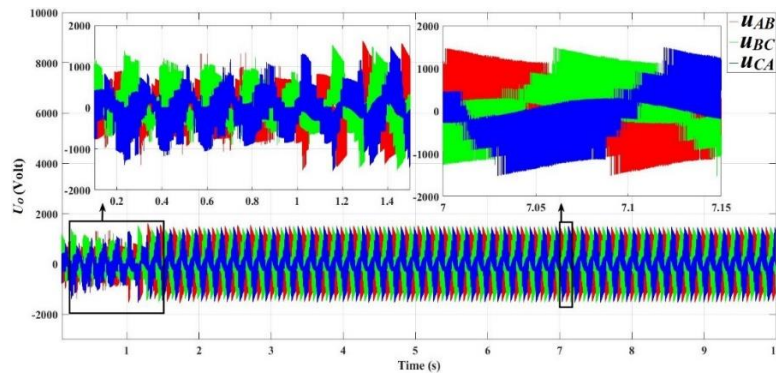

Figure 26. Converter output voltages

Table 2 shows a lower values of peak-to-peak voltage ripple of SM capacitor of the hybrid MMC compared with the traditional MMC, this because of the series switch, reducing the average arm voltage of the MMC, leading to reduce the storage energy in the SM capacitor.

Table 2. SM capacitor voltage ripple

Speed (rpm)	Traditional MMC	Hybrid MMC
1189 rpm	55 V	55 V
200 rpm	432 V	140 V
100 rpm	860 V	170 V

5.   CONCLUSION

This paper introduced a hybrid MMC to drive the induction motor. The results show that the ability of hybrid MMC to drive the induction motor at constant load torque with wide speed range. Compared with the traditional MMC, the hybrid MMC exhibits lower peak-to-peak voltage ripple of the SM capacitor without increasing the capacitor value as shown in the simulation results when the induction motor is operated at low speed. The motor can be operated with very low speed of 100rpm with peak-to-peak capacitor voltage ripple of 170V compared with high value of 860V in traditional system. A suitable control is introduced for the hybrid MMC in order to minimize the peak-to-peak voltage ripple of capacitor and to obtain high-quality sinusoidal waveform of the induction motor current without using any additional filter.

REFERENCES

[1]   A. U. Lawan, H. A. F. Almurib, and J. G. Khor, "Modular multilevel converter (MMC) based STATCOM with vector control and virtual impedance voltage compensations," *Int. J. Power Electron. Drive Syst.*, vol. 10, no. 4, p. 1833, Dec, 2019.
[2]   H. Attia and A. Sagafinia, "Novel discrete components based speed controller for induction motor," *Int. J. Power*

Electron. Drive Syst., vol. 7, no. 4, pp. 1075–1084, Dec, 2016.

[3]   A. Lesnicar and R. Marquardt, "An innovative modular multilevel converter topology suitable for a wide power range," in *2003 IEEE Bologna Power Tech Conference Proceedings,* vol. 3, pp. 6-pp, Jun. 2003.

[4]   M. A. Perez, S. Bernet, J. Rodriguez, S. Kouro, and R. Lizana, "Circuit topologies, modeling, control schemes, and applications of modular multilevel converters," *IEEE Trans. Power Electron.*, vol. 30, no. 1, pp. 4–17, Jan. 2015.

[5]   S. Debnath, J. Qin, B. Bahrani, M. Saeedifard, and P. Barbosa, "Operation, control, and applications of the modular multilevel converter: A review," *IEEE Trans. power Electron.*, vol. 30, no. 1, pp. 37–53, Jun. 2015.

[6]   S. Rohner, S. Bernet, M. Hiller, and R. Sommer, "Modulation, losses, and semiconductor requirements of modular multilevel converters," *IEEE Trans. Ind. Electron.*, vol. 57, no. 8, pp. 2633–2642, Aug. 2010.

[7]   G. Bergna *et al.*, "An energy-based controller for HVDC modular multilevel converter in decoupled double synchronous reference frame for voltage oscillation reduction," *IEEE Trans. Ind. Electron.*, vol. 60, no. 6, pp. 2360–2371, Jun. 2013.

[8]   C. Oates, "Modular multilevel converter design for VSC HVDC applications," *IEEE J. Emerg. Sel. Top. Power Electron.*, vol. 3, no. 2, pp. 505–515, Jun. 2015.

[9]   N. Ahmed *et al.*, "HVDC SuperGrids with modular multilevel converters - The power transmission backbone of the future," *Int. Multi-Conference Syst. Signals Devices, SSD 2012 - Summ. Proc.*, Mar. 2012.

[10]   H. Akagi, "Classification, terminology, and application of the modular multilevel cascade converter (MMCC)," *IEEE Trans. Power Electron.*, vol. 26, no. 11, pp. 3119–3130, Nov. 2011.

[11]   S. Rohner, M. Hiller, and R. Sommer, "A new highly modular medium voltage converter topology for industrial drive application," in *Power electronics and applications, EPE 13th European conference*, Oct. 2009.

[12]   G. J. M. De Sousa and M. L. Heldwein, "Modular multilevel converter based unidirectional medium/high voltage drive system," *IECON Proc. (Industrial Electron. Conf.*, pp. 1037–1042, Nov. 2013.

[13]   M. Spichartz, V. Staudt, and A. Steimel, "Modular multilevel converter for propulsion system of electric ships," in *2013 IEEE Electric Ship Technologies Symposium (ESTS)*, pp. 237–242, Apr. 2013.

[14]   M. Hagiwara, K. Nishimura, and H. Akagi, "A medium-voltage motor drive with a modular multilevel PWM inverter," *IEEE Trans. Power Electron.*, vol. 25, no. 7, pp. 1786–1799, Jul. 2010.

[15]   J. E. Huber and A. J. Korn, "Optimized pulse pattern modulation for modular multilevel converter high-speed drive," *15th Int. Power Electron. Motion Control Conf. Expo. EPE-PEMC 2012 ECCE Eur.*, pp. 1–7, Sep. 2012.

[16]   B. Li, R. Yang, D. Xu, G. Wang, W. Wang, and D. Xu, "Analysis of the phase-shifted carrier modulation for modular multilevel converters," *IEEE Trans. Power Electron.*, vol. 30, no. 1, pp. 297–310, Jan. 2015.

[17]   S. Kouro *et al.*, "Recent advances and industrial applications of multilevel converters," *IEEE Trans. Ind. Electron.*, vol. 57, no. 8, pp. 2553–2580, Aug. 2010.

[18]   M. Malinowski, K. Gopakumar, J. Rodriguez, and M. A. Perez, "A survey on cascaded multilevel inverters," *IEEE Trans. Ind. Electron.*, vol. 57, no. 7, pp. 2197–2206, Jul. 2010.

[19]   B. Li *et al.*, "An improved circulating current injection method for modular multilevel converters in variable-speed drives," *IEEE Trans. Ind. Electron.*, vol. 63, no. 11, pp. 7215–7225, Nov. 2016.

[20]   M. Hagiwara, K. Nishimura, and H. Akagi, "A medium-voltage motor drive with a modular multilevel PWM inverter," *IEEE Trans. Power Electron.*, vol. 25, no. 7, pp. 1786–1799, 2010.

[21]   A. Antonopoulos, L. Ängquist, L. Harnefors, and H. P. Nee, "Optimal selection of the average capacitor voltage for variable-speed drives with modular multilevel converters," *IEEE Trans. Power Electron.*, vol. 30, no. 1, pp. 227–234, Jan. 2015.

[22]   H. Peng, M. Hagiwara, and H. Akagi, "Modeling and analysis of switching-ripple voltage on the DC link between a diode rectifier and a modular multilevel cascade inverter (MMCI)," *IEEE Trans. Power Electron.*, vol. 28, no. 1, pp. 75–84, Jan. 2013.

[23]   B. Li, S. Zhou, D. Xu, S. J. Finney, and B. W. Williams, "A Hybrid Modular Multilevel Converter for Medium-Voltage Variable-Speed Motor Drives," *IEEE Trans. Power Electron.*, vol. 32, no. 6, pp. 4619–4630, Jun. 2017.

[24]   S. Zhou, J. Wang, B. Li, and D. Xu, "Capacitor Voltage Ripple Reduction of Hybrid Modular Multilevel Converter Based on Third-Harmonic Injection," *ICEMS 2018 - 2018 21st Int. Conf. Electr. Mach. Syst.*, pp. 2216–2220, May. 2019.

[25]   S. Zhou, B. Li, M. Guan, X. Zhang, Z. Xu, and D. Xu, "Capacitance Reduction of the Hybrid Modular Multilevel Converter by Decreasing Average Capacitor Voltage in Variable-Speed Drives," *IEEE Trans. Power Electron.*, vol. 34, no. 2, pp. 1580–1594, Feb. 2019.

[26]   B. Li, R. Li, B. W. Williams, and D. Xu, "Energy transfer analysis for capacitor voltage balancing of modular multilevel converters," *2016 IEEE Transp. Electrif. Conf. Expo, ITEC 2016*, no. Mmc, Jun. 2016.

[27]   G. Liu, Q. Jiang, and Y. Wei, "Study on capacitor voltage balancing control of modular multilevel converter at low frequency," *Int. J. Comput. Electr. Eng.*, vol. 5, no. 2, p. 196, Apr. 2013.

[28]   Y. S. Kumar and G. Poddar, "Medium-voltage vector control induction motor drive at zero frequency using modular multilevel converter," *IEEE Trans. Ind. Electron.*, vol. 65, no. 1, pp. 125–132, Jan. 2018.

[29]   A. M. Nori and T. K. Hassan, "Modeling and simulation of quasi-Z-source indirect matrix converter for permanent magnet synchronous motor drive," *Int. J. Power Electron. Drive Syst.*, vol. 10, no. 2, pp. 882–899, June, 2019.

[30]   B. Wu and M. Narimani. *High-power converters and AC drives*. John Wiley & Sons, May, 2017.

[31]   M. Hagiwara, R. Maeda, and H. Akagi, "Control and analysis of the modular multilevel cascade converter based on double-star chopper-cells (MMCC-DSCC)," *IEEE Trans. Power Electron.*, vol. 26, no. 6, pp. 1649–1658, Jun. 2011.